

An Optimization Algorithm for Human Joint Angle Time-History Generation Using External Force Data

CLAUDIA MAZZÀ and AURELIO CAPPOZZO

Dipartimento di Scienze del Movimento Umano e dello Sport, Istituto Universitario di Scienze Motorie,
Piazza Lauro de Bosis 6, 00194 Rome, Italy

(Received 23 April 2003; accepted 29 December 2003)

Abstract—A mathematical model is presented that estimates joint kinematics and kinetics using measured external resultant loads and readily available parameters. The musculo-skeletal system was represented by a planar three degrees of freedom open kinematic chain. Information extraction was limited to the flexion–extension function of ankle, knee, and hip during quasi-planar motor tasks. Starting from plausible first approximation kinematics, other kinematic functions are iteratively generated by an optimization algorithm and corresponding ground reaction loads are calculated through inverse dynamics. Kinematic coordinates are represented using B-splines and modified by manipulating the control points. The iterative procedure stops and provides the final kinematic and kinetic estimates when a similarity criterion between estimated and measured ground reaction components is satisfied. The model structure was elaborated upon and the algorithm parameters optimized for robustness and accuracy using a benchmark motion in a simulation exercise. The maximal root mean square difference over time between estimated and benchmark quantities was approximately 1% of the peak to peak value for ground reaction components and intersegmental couples, and 6% for joint angles.

Keywords—Biomechanical model, Joint kinematics, Ground reactions.

INTRODUCTION

Human movement analysis aims to gather information concerning the relative movement between adjacent bones (joint kinematics), and the forces and couples exchanged with the environment (external loads) or between body segments (intersegmental loads). The quantities that provide this information are either measured or estimated. Normally, the measured quantities are skin point instantaneous positions obtained using stereophotogrammetry, external forces measured using dynamometers, and anthropometric quantities. The quantities that are not directly observable are estimated using an anthropomorphic model that consists of a kinematic chain of links, each of which representing

a body segment, that are considered non-deformable. The number of links and constraints imposed by the joints determines the number of degrees of freedom of the model and define the limits within which functional information can be extracted.^{11,21}

When estimating intersegmental loads, both the variables that allow for the description of the motion of the musculo-skeletal model and of the resultant external reaction forces and couples acting on it are often measured. This is done even when the former variables would allow for the estimation of the latter variables through the equations of motion (solution of the inverse dynamics problem as applied to an open kinematic chain). Economic considerations are put aside for the sake of accuracy. In actuality, the measured forces are normally far more reliable than the estimated forces, which may be affected by root mean square errors up to 15–20%.³ This inaccuracy is associated with the discrepancy between the selected mechanical model and the real system, with the errors that affect the model parameters and the model link instantaneous position and orientation, and with the fact that velocities and accelerations are computed from noisy data.^{2,11} Kuo¹⁴ further exploited the above-mentioned information redundancy and improved the estimate of the intersegmental couples of a planar, three degrees of freedom, musculo-skeletal model by writing over-determinate equations of motion and solving them using an optimization approach. This approach, based on a weighted least-squares technique, minimized the difference between measured and estimated external loads.

The above considerations and the fact that dynamometers are relatively inexpensive and easy-to-use experimental apparatuses^{3,10} gave rise to the following question: given a mechanical model of the musculo-skeletal system, is it possible to estimate its kinematics and kinetics, during the execution of a physical exercise, starting from the knowledge of the time course of the resultant external reaction load and other readily available parameters? The analytical formulation of this problem may be determinate or indeterminate, depending on the number of degrees of freedom of the mechanical model used. However, even when the problem

Address correspondence to Claudia Mazzà, Dipartimento di Scienze del Movimento Umano e dello Sport, Istituto Universitario di Scienze Motorie, Piazza Lauro de Bosis 6, 00194 Rome, Italy. Electronic mail: mazzà@iusm.it

is determinate, generally no analytical closed-form solution exists for it.²⁰ In the latter case, the equations of motion are integrated numerically and a solution can be sought through an iterative procedure that provides no clue about how far the chosen solution is from the real one. Optimization algorithms are preferable since they intrinsically provide an objective criterion to quantify the “quality” of the achieved solution. In addition, in principle, they can cope with problems that are intrinsically mathematically indeterminate.²²

Levin *et al.*¹⁵ dealt with the above-mentioned question while attempting to determine the intersegmental loads at the lower limb joints during the maintenance of an up-right posture. They used a three-dimensional, two degrees of freedom model driven by the ground reactions acting on each foot. The kinematic coordinates involved were iteratively varied and, for each set of their values, the external forces were estimated. The coordinates for which the difference between the measured and estimated external forces was minimal were taken as solutions of the algorithm. The algorithm exhibited convergence difficulties and showed a low reliability of the estimated external medio-lateral force and antero-posterior couple vector components. The estimated kinematic variables were not validated using some independent observation.

This paper deals with a mathematical model, named JAGO (joint angles generation using optimization), that addresses the above-mentioned question. The JAGO model structure, based on an optimization algorithm, is elaborated upon and optimal values of the algorithm parameters are derived to achieve its robustness and result accuracy. An analytically simulated motion, for which exact kinematics and kinetics are assumed to be known, is used to assess the model performance. The paper concentrates on the mathematical model and does not discuss the other factors that may affect the overall performance of the method when experimental data are used.³

The JAGO model is based on a three degrees of freedom mechanical model of the musculo-skeletal system. It is conceived to provide information about joint kinematics and kinetics in a selected plane. This means that movements that are quasi-symmetric relative to the sagittal plane and with a fixed base of support are mostly coped with. Squatting and rising from a seat are typical examples of a motor act in which asymmetries in the frontal plane may carry no interest for the analyst.^{12,19} Despite these limitations, similar mechanical models have been extensively used both in heuristic^{7,13,18} and application contexts.¹⁷ However, this was done in conjunction with both stereophotogrammetry and dynamometry.

THE JAGO MODEL

The Mechanical Model

The JAGO model uses a mechanical model of the human body that consists of a planar open kinematic chain made

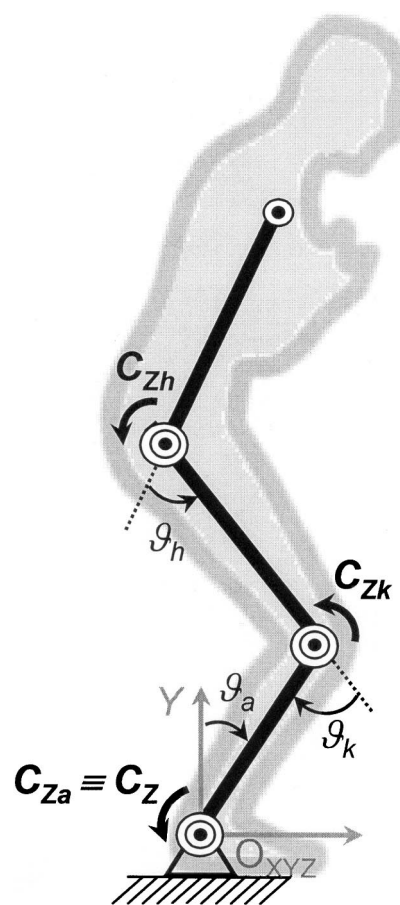


FIGURE 1. Mechanical model of the musculo-skeletal system (three-link, planar open kinematic chain).

of mono-dimensional rigid links connected by hinges. One end of the linkage is free to move in space, while the other interacts with the environment at a known point where it is subjected to the action of an external reaction force, the line of action of which passes through that point, and a couple. Subject specific inertial (mass, location of the centre of mass, mass moment of inertia) and geometrical parameters are associated with each modelled body segment.

The three links of the model represented the shanks, the thighs, and the upper part of the body that incorporates the head, the arms, and the trunk (the so-named HAT) (Fig. 1). They were joined by cylindrical hinges endowed with muscle equivalent rotational actuators, and located at points approximating the ankle, knee, and hip joint centres. The relevant three degrees of freedom were described using the joint angles indicated in Fig. 1. With this model, motor acts may be analyzed during which head and upper limbs may be considered to be stationary with respect to a virtually rigid trunk and the ankle joint stationary with respect to the ground (motionless foot). The ground reaction (GR) force and couple vectors were reduced to the stationary ankle joint centre and were represented by the following components: vertical (Y) and antero-posterior (X) force components and

the medio-lateral (Z) couple vector component, relative to a laboratory fixed set of axes consistent with the subject's anatomical planes (Fig. 1). From now on, the GRs are supposed to coincide with the ankle intersegmental loads.

The Mathematical Model

The JAGO mathematical model receives as input the following quantities:

- measured pattern versus time of the GR components;
- measured initial and final (boundary) values of the ankle, knee, and hip joint angles;

- expected range of variation of the joint angular position, velocity, and acceleration (minimum and maximal values);
- subject's body segment inertial and geometric parameters as obtained using regression equations and easy to measure anthropometric quantities.

The objective of the model is to provide estimates of the kinematics (angles). This is done using the following procedure (Fig. 2). For each type of motor task, the model is provided with arbitrary first approximation functions (FAFs) representing plausible time histories of the three joint-angles. Before being used, FAFs are forced to

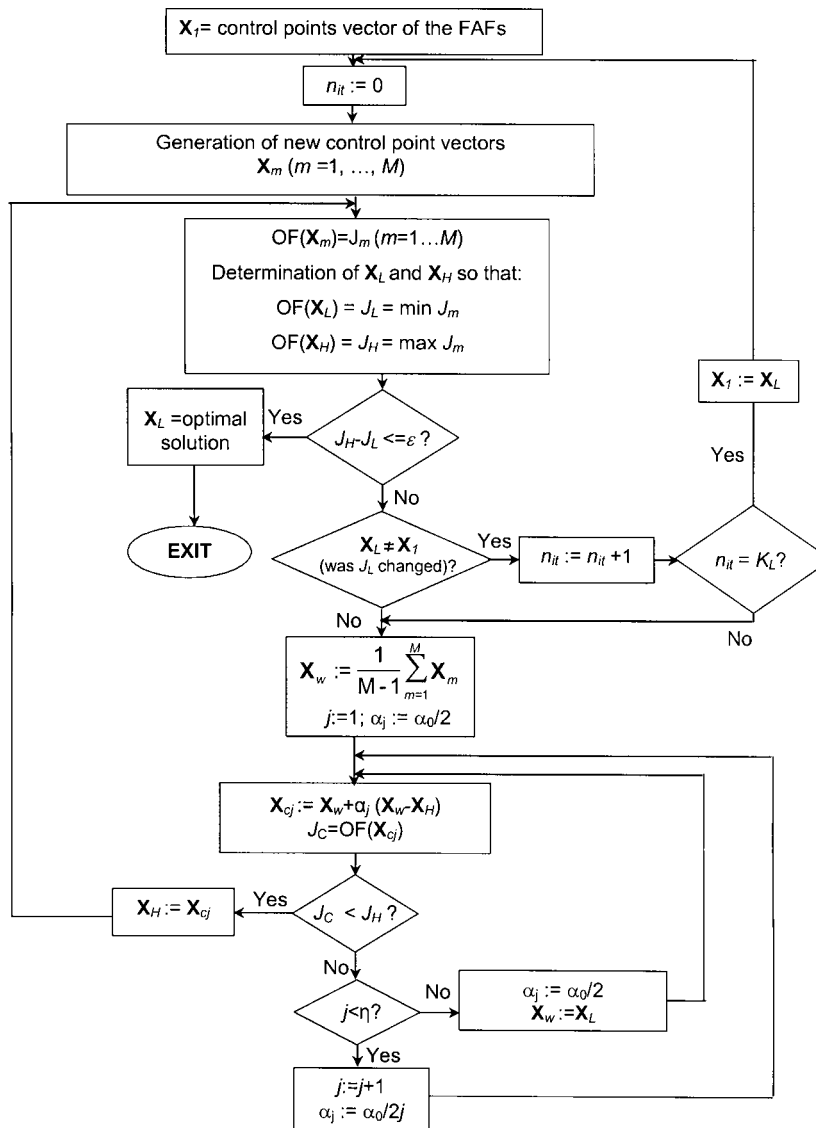


FIGURE 2. Scheme of the optimization algorithm. n_i is a counter for the number of iterations, K_L denotes the maximum number of times that the algorithm can iterate before re-generating the control point vectors, ε the threshold below which the difference between the maximal and minimal value assumed by the objective function for the generated control point vectors is considered negligible (and the algorithm stops iterating), α_0 the basis value for the parameter α_j , which defines the vector X_{Cj} , η the upper threshold for j , and M the number of control point vectors X_m generated. Values chosen in the present study were $K_L = 3000$, $\varepsilon = 10^{-4}$, and, after Box,¹ $\eta = 10^4$, $\alpha_0 = 2.6$.

be consistent with the initial and final joint angle values. Starting from the FAFs, other functions are iteratively generated by an optimization algorithm and the corresponding ground reaction forces and couples are calculated through inverse dynamics. The Newton–Euler method was used for the inverse dynamic computation. When a similarity criterion, detailed below, that includes the estimated and the measured GR components is met, this iterative procedure stops, and the final kinematic and kinetic estimates are provided.

Each Cartesian joint angle time history ($\theta = \theta(t)$; $t \in [0, 1]$) was analytically represented using B-splines.¹⁶ These are piecewise polynomial functions (basis functions) of order k [degree $(k - 1)$] joined $[C^{k-2}]$ continuously at points on the curve that correspond to specified values of a parameter referred to as knots. In the present study, this parameter was made to coincide with the independent variable normalized time and these values give place to the so-named knot sequence ($|t_i|$, $i = 0, \dots, T$; $t_i \leq t_{i+1}$). Given this vector and the order k , the above-mentioned basis functions are recursively generated^{6,9}:

$$\begin{aligned} N_{i,1}(t) &= 1, \quad \text{for } t_i \leq t \leq t_{i+1} \\ N_{i,1}(t) &= 0, \quad \text{elsewhere} \\ N_{i,k}(t) &= \frac{(t - t_i)N_{i,k-1}(t)}{t_{i+k-1} - t_i} + \frac{(t_{i+k} - t)N_{i+1,k-1}(t)}{t_{i+k} - t_{i+1}}. \end{aligned} \quad (1)$$

These functions are zero outside the interval $t \in t_i, t_{i+k}$ and $N_{i,k} \in [0, 1]$. They are determined entirely by the relative spacing between the knots. The B-spline function is represented as a linear combination of $N + 1$ basis functions each weighted by the following control points θ_i , $i = 0, \dots, N$:

$$\theta(t) = \sum_{i=0}^N \theta_i \cdot N_{i,k}(t), \quad t \in [t_k, t_{N+1}]. \quad (2)$$

The B-spline approximates the polygon constructed using the control points (Fig. 3). Note that the above-mentioned parameters are related by the following relationship: $N + k + 1 = T$.

The first and last k knots were made to coincide (multiplicity k). This entailed that the B-spline interpolated the first and last control points. The other knots were equally spaced giving place to an ‘‘open uniform’’ B-spline. Given an order k , the knot sequence was kept constant and all manipulations of the target functions $\theta(t)$ were made by acting on the values of the control points (control handles). The overall model joint kinematics were represented using a control point vector, $\mathbf{X} = |X_i|$, $i = 0, \dots, 3 \cdot N + 3$, constructed by putting in series the control points θ_i that represented the three joint angle time functions.

At each iteration of the optimization algorithm, different joint trajectories were generated by modifying a seed control vector \mathbf{X}_1 , which resulted from the previous iteration—

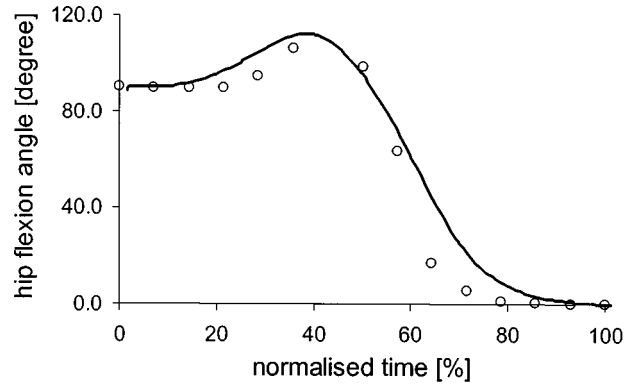


FIGURE 3. The hip joint angle represented using a sixth order B-spline, with $N + 1 = 15$. Control points (empty circles) are also indicated. The following knot vector sequence was used: $[0 \ 0 \ 0 \ 0 \ 0 \ 10 \ 20 \ 30 \ 40 \ 50 \ 60 \ 70 \ 80 \ 90 \ 100 \ 100 \ 100 \ 100 \ 100 \ 100]$.

or, at the beginning of the process, represented the FAFs— into a preset number (M) of vectors \mathbf{X}_m of control points:

$$\mathbf{X}_m = \mathbf{X} + \mathbf{D} \times \mathbf{r}_m, \quad m = 1, \dots, M \quad (3)$$

where \mathbf{r}_m is a uniform random vector with elements in the range ± 1 and \mathbf{D} is a vector of scaling factors set so that the resulting joint trajectories are consistent with the admissible ranges of joint angular position.

The above-mentioned similarity criterion was represented by an objective function (OF) which embedded the root mean square (r.m.s.) differences between the measured and estimated GR components (δ_{FX} , δ_{FY} , δ_{CZ}), calculated over the observation time interval, respectively. Time derivatives, inherent in inverse dynamics, posed no problem given the analytical representation of movement data. In order to avoid the local concentration of these differences, the entire motor act duration was divided into n intervals and the above-defined r.m.s. differences computed for each of them (δ_{FX_i} , δ_{FY_i} , δ_{CZ_i} ; $i = 1, \dots, n$). Thereafter, the following quantities were defined

$$\begin{aligned} J_{FX} &= \delta_{FX} + \sum_{i=1}^n |\delta_{FX} - \delta_{FX_i}|, \quad J_{FY} = \delta_{VF} + \\ &\sum_{i=1}^n |\delta_{FY} - \delta_{FY_i}|, \quad J_{CZ} = \delta_{CZ} + \sum_{i=1}^n |\delta_{CZ} - \delta_{CZ_i}|, \end{aligned} \quad (4)$$

and their weighted sum calculated:

$$J = w_{FX} J_{FX} + w_{FY} J_{FY} + w_{CZ} J_{CZ}. \quad (5)$$

The terms w_{FX} , w_{FY} , w_{CZ} are weighting coefficients that allow to modulate the tie between the OF and the r.m.s. difference of each of the three GR components. The values of these coefficients are set empirically depending on the characteristics of the motor act under analysis (in the present study $w_{FX} = 2$; $w_{FY} = 1$; $w_{CZ} = 3$).

For each \mathbf{X}_m , generated as illustrated above, an objective function J_m ($m = 1, \dots, M$) was calculated. The minimum

and maximum of J_m , referred to as J_L and J_H , respectively, were identified, together with the two relevant vectors \mathbf{X}_L and \mathbf{X}_H . If $J_L - J_H$ was lower than a preset threshold (ϵ), then the optimal solution was found, otherwise the following iterative procedure, based on the Complex Method,¹ was started. If \mathbf{X}_L did not coincide with the seed vector \mathbf{X}_1 , then it was made to take the place of the latter vector and the process was reiterated. On the contrary, another seed vector had to be searched for that would have allowed the algorithm to reach its optimal solution. The centroid (\mathbf{X}_w) of the vectors \mathbf{X}_m , but \mathbf{X}_H , was calculated as indicated in Fig. 2. Based on \mathbf{X}_w , other vectors \mathbf{X}_{c_j} and corresponding J_{c_j} were iteratively calculated, until a J_{c_j} lower than J_H was found. \mathbf{X}_H was then replaced with \mathbf{X}_{c_j} and the process started again. If the latter circumstance did not occur, then \mathbf{X}_w was substituted by \mathbf{X}_L and the process was made to start again.

Model Parameters

The parameters of the mathematical model are (1) the order k and the number ($N + 1$) of control points of the B-splines used to represent the joint angle time functions, (2) the number M of functions that are generated at each iteration by the optimization algorithm, and (3) parameters that describe the discrepancy between the FAFs and the true joint angle time histories. To the latter purpose the mean values of the r.m.s. differences (\bar{d}), expressed in percent, and of the correlation coefficients (\bar{c}) calculated between the reference trajectories of each of the three joints and the relevant FAFs, were used.

THE SIMULATION

The simulation process designed to tune JAGO's intrinsic parameters and assess its performance is summarized in Fig. 4.

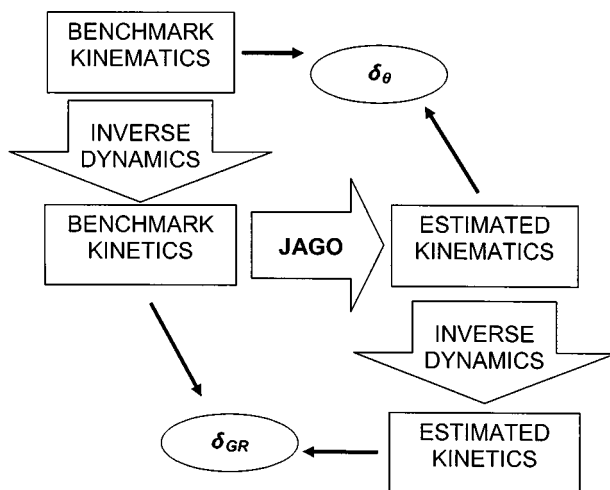


FIGURE 4. Flow chart of the simulation.

Benchmark kinematic variables were derived from experimental data. Ten young adult subjects (five males and five females) were asked to perform, in a free fashion, a semi-tucked to erect standing exercise with their arms folded across their chest (each referred to as “trial”). The marker set recommended in Davis *et al.*⁸ was used. Marker trajectories were reconstructed using a nine camera VICON system 612 (120 frames/s). Ten sets of the right ankle, knee, and hip flexion–extension angle analytical time functions (benchmark kinematics) and the distances between these joint centres were calculated from marker position data and associated with the mechanical model depicted in Fig. 1.

The subject specific inertial parameters were estimated using the regression equations given by Winter.²³ The GRs and the knee and hip intersegmental forces and couples (benchmark kinetics) were calculated using the benchmark kinematics through inverse dynamics (Fig. 4). Since kinematic quantities were represented analytically, double differentiation posed no problem.

The joint angle boundary values were derived from the benchmark kinematics. FAFs were constructed by manipulating the control point vector obtained using the data of a trial chosen at random. One hundred different FAFs were generated that differed from the selected benchmark kinematic functions measured by values of \bar{d} in the range 0.9–23% and of \bar{c} in the range 0.77–0.97.

The benchmark GR components, the mechanical model parameters, and the kinematic boundary values were fed to the JAGO model in the configuration to be tested. Since the procedure that iteratively generates the kinematic coordinates is intrinsically random, given a set of input variables and a set of FAFs, the JAGO model output was not repeatable. Thus, in order to assess this aspect, each simulation was repeated 10 times using the same data (each referred to as “run”).

Estimated and benchmark kinematics and GR variables were compared using the following quantities:

1. the r.m.s. difference over time between the benchmark joint angles and GRs and the corresponding estimated functions for each run of all trials; all of these values were expressed as percentage of the peak to peak value of the relevant benchmark function (δ_{θ_a} , δ_{θ_k} , δ_{θ_h} and δ_{FX} , δ_{FY} , δ_{CZ});
2. the average values of the latter kinematic and kinetic r.m.s. differences (δ_{θ} and δ_{GR} , respectively);
3. the average value, over the 10 runs of each trial, of the r.m.s. differences defined in items “a” and “b” (e_{θ_a} , e_{θ_k} , e_{θ_h} , e_{FX} , e_{FY} , e_{CZ} , e_{θ} , and e_{GR}) and the relevant standard deviations (SD);
4. descriptive statistics of e_{θ_a} , e_{θ_k} , e_{θ_h} , e_{FX} , e_{FY} , e_{CZ} , e_{θ} , and e_{GR} estimated over the 10 trials (\bar{e} and relevant SD).

The JAGO model was tested under different configurations. The motor act duration was first divided into $n = 3$ intervals. With respect to the B-splines, the order k was given

the values 4 (minimum value to allow for second derivative continuity) to 6 and the number $N + 1$ of the control points the values 15 and 30. These configurations were tested with the other parameters set at conservative values ($\bar{d} = 6.5\%$, $\bar{c} = 0.99$, $M = 800$). In order to assess the dependence of the model performance on the FAFs, the simulation was carried out first by selecting the FAFs, from the previously mentioned hundred functions that exhibited a virtually constant \bar{d} , with values equal to $20 \pm 2\%$, and then using those that exhibited a virtually constant \bar{c} , with values equal to 0.97 ± 0.02 . The other parameters had the following values: $M = 400$, $k = 6$, $N + 1 = 15$. The sensitivity of the algorithm to the parameter M was assessed by varying M over the range 50–900 (step 50), while $\bar{d} = 6.5\%$, $\bar{c} = 0.99$, $k = 6$, and $N + 1 = 15$. For selected JAGO model configurations, the errors that affected hip and knee intersegmental couples, calculated using estimated kinematics and benchmark GRs, e_{CZk} , and e_{CZh} , were also assessed. Finally, selected tests were carried out dividing the motor act duration into $n = 7$ and 15 intervals.

RESULTS

Model Parameter Analysis

Kinematic and kinetic quantities estimated using sixth order B-splines with 15 control points yielded better results ($\bar{e}_{GR} = 0.40 \pm 0.30\%$ and $\bar{e}_{\theta} = 2.00 \pm 1.50\%$) than fifth order splines ($\bar{e}_{GR} = 0.60 \pm 0.30\%$ and $\bar{e}_{\theta} = 4.01 \pm 1.30\%$) or fourth order splines ($\bar{e}_{GR} = 0.72 \pm 0.27\%$ and $\bar{e}_{\theta} = 4.65 \pm 1.34\%$) without requiring a significantly higher computation time. The use of sixth order splines with 30 control points required an almost doubled computation time and led to results comparable with those obtained with 15 control points. Thus, sixth order B-splines with 15 control points are recommended and used from here on.

Figure 5 shows the results (δ_{θ} , δ_{GR}) of the simulations performed using different FAFs and one randomly selected trial. Other trials yielded similar results. Data dispersion in these graphs reflects the above-mentioned random component of the algorithm. This aspect will be dealt with later. It appears evident that the greater the correlation coefficient (\bar{c}) between FAFs and true joint angle time functions the better the performance of the algorithm. The slope (regression coefficient) of the relevant regression lines was found to be approximately -100 . This means that if \bar{c} is decreased by 0.1, the error increases by about 10%. Note that the large errors exhibited in Fig. 5(a) are due to the large mean r.m.s. difference ($\bar{d} = 20 \pm 2\%$). The value of \bar{d} , in fact, did not drastically affect the reliability of the kinematic and kinetic estimates provided that it was given a value less than 15% [Fig. 5(b)]. However, as soon as \bar{d} became higher than 15%, the inaccuracy of the results increased sharply.

Figure 6 shows the dependence of e_{θ} and e_{GR} and the relevant SD from the parameter M . The estimated angle

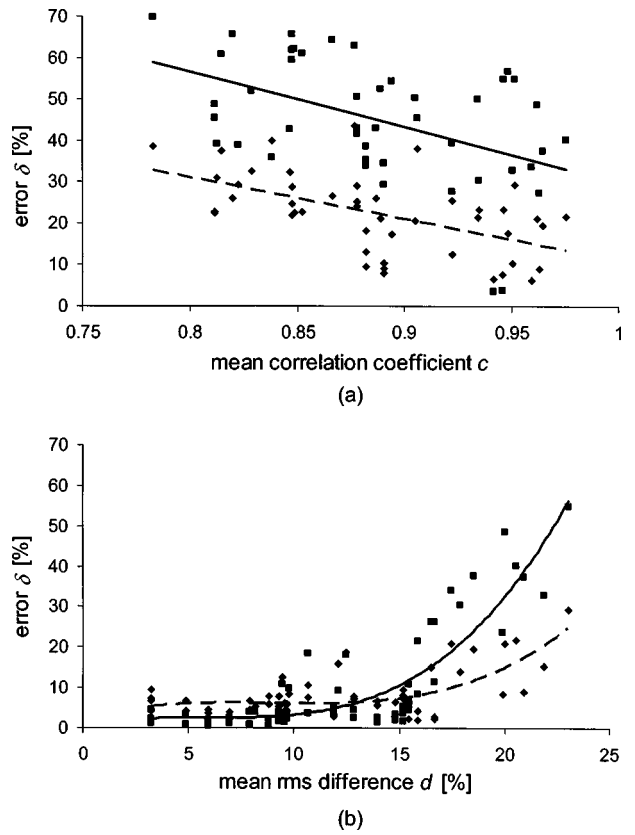


FIGURE 5. Results (δ_{θ} : dashed line and diamonds; δ_{GR} : full line and squares) of a simulation ($M = 400$, $k = 6$, $N + 1 = 15$) carried out with different first approximation functions and relative to a trial chosen at random. FAFs were selected in order to have virtually constant \bar{d} ($20 \pm 2\%$), and a \bar{c} varying in the range 0.77–0.97 [graph (a)], or a virtually constant \bar{c} (0.97 ± 0.02), and a \bar{d} varying in the range 0.9–23% [graph (b)]. Relevant regression curves are also reported. These exhibited the following correlation coefficients and standard errors: $\delta_{\theta} = f(\bar{c})$, $r^2 = 0.28$, SE = 8.1%; $\delta_{GR} = f(\bar{c})$, $r^2 = 0.22$, SE = 13%; $\delta_{\theta} = f(\bar{d})$, $r^2 = 0.77$, SE = 9.2%; $\delta_{GR} = f(\bar{d})$, $r^2 = 0.44$, SE = 4.9%.

accuracy remarkably improved for $M > 500$ and stabilized thereafter. In addition, errors in the model output became more repeatable (reduced SD). The inaccuracy that affected the ankle angle ($e_{\theta a}$) was about twofold with respect to that affecting the other two joint angles ($e_{\theta k}$, $e_{\theta h}$) for any value of M .

According to the above results, the following values are recommended for the intrinsic parameters: FAFs with $\bar{d} < 15\%$ and $\bar{c} > 0.90$ and $M > 500$. These values of \bar{d} and \bar{c} are feasible in practice. In fact relevant values calculated with reference to the 10 angle time functions obtained experimentally fell within the indicated ranges.

Some of the tests illustrated above, carried out with the motor act duration divided into $n = 3$ intervals, were repeated with $n = 7$ and 15, which is the recommended number of control points. As n increased, the values of e_{θ} and e_{GR} decreased by a maximum of 20% and computing time

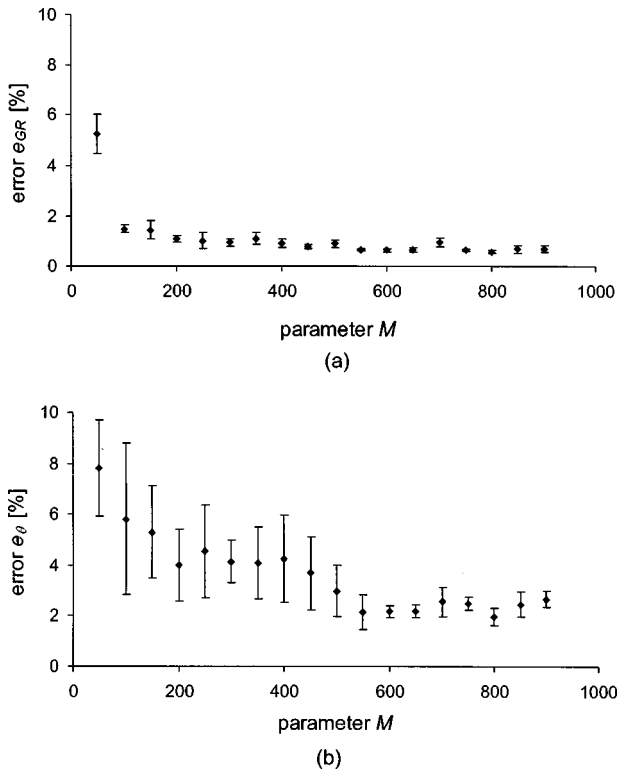


FIGURE 6. Algorithm response to changes of the number M of control vectors generated at each iteration ($\bar{d} = 6.5\%$, $\bar{c} = 0.99$, $k = 6$, and $N + 1 = 15$). The errors e_θ and e_{GR} (\pm SD) were computed using the data of a randomly chosen trial and over 10 different runs.

exhibited no detectable change. Values obtained for the errors e and relevant SD, relative to each joint angle and GR component, are shown in Table 1.

The analyses reported below were obtained by setting the parameters at values consistent with the above limits. Relevant computing time for each run, on a 2.2 GHz Intel

Pentium IV CPU, with a 512 Mb RAM, was, on average, 55 min.

Model Precision and Accuracy Evaluation

The precision of the JAGO estimates has already been alluded to while dealing with its sensitivity to the parameter M . Using parameter values that satisfied the illustrated criteria ($n = 15$, $\bar{d} = 10\%$, $\bar{c} = 0.97$, $M = 800$), the SD of the quantities e_θ and e_{GR} computed for the 10 runs of a randomly selected trial resulted in values of 0.65 and 0.06%, respectively. The SD were equally distributed among the GR components, while the same could not be stated for the ankle, knee, and hip kinematics: the SD for these three angles were 2.1, 1.5, and 0.7%, respectively.

The overall performance of the algorithm was evaluated by averaging the results obtained over the 10 trials and using FAFs characterized by $\bar{d} = 13.3 \pm 1.3\%$ and $\bar{c} = 0.93 \pm 0.03$, and $n = 15$ and $M = 800$. Results showed a remarkable accuracy for the estimates of the GR components ($\bar{e}_{GR} = 0.40 \pm 0.3\%$). The joint angles exhibited an $\bar{e}_\theta = 1.73 \pm 1.4\%$. No differences among the errors in the estimates of the three GR components were found. The largest joint angle error was exhibited at the ankle ($\bar{e}_{\theta_a} = 2.75 \pm 2.42\%$), whereas the error at the hip was the smallest ($\bar{e}_{\theta_h} = 1.15 \pm 1.31\%$).

Figure 7 depicts examples of results that were obtained by the JAGO model when used with feasible parameters.

The intersegmental couples at the hip and knee, calculated using the estimates yielded by the above-mentioned trials, exhibited errors in the following ranges: $\bar{e}_{CZ_h} = 0.61 \pm 0.49\%$ and $\bar{e}_{CZ_k} = 0.64 \pm 0.42\%$, respectively.

DISCUSSION

The objective of this study was to assess the performance of a method that estimates the kinematics and kinetics in the ankle, hip, and knee joints from force plate data based on the use of a multi-segmental model of the human body and an optimization algorithm. A question arose as to whether a correct functioning of the optimization algorithm was affected by the choice of its internal parameters. Optimal values of these parameters were found.

The proposed algorithm proved to be robust in that in all tests performed always converged to a solution. It was demonstrated that a proper choice of the B-spline order is basic, whereas the increment of the control points number of the B-spline over 15 does not enhance the quality of the kinematics reconstruction, but only affects computation time. By using a number M , of kinematic functions iteratively generated by the algorithm, greater than 500 results improve remarkably. Another crucial factor that has to be considered in order to get reliable joint kinematics reconstructions is the choice of the FAFs and their correlation with the actual functions. The r.m.s. difference between the

TABLE 1. Mean (e) and standard deviation (SD) of the errors that affect the estimates of the ground reaction components and the hip, knee, and ankle angles obtained with $n = 15$, $\bar{d} = 10\%$, $\bar{c} = 0.97$, $M = 800^a$

	e (SD) [%]
<i>GR component</i>	
FX	0.5 (0.1)
FY	0.5 (0.0)
CZ	0.5 (0.1)
<i>Angle</i>	
θ_a	2.7 (0.3)
θ_k	0.8 (0.1)
θ_h	1.6 (0.2)

^aResults relative to a randomly chosen trial and averaged over 10 different runs.

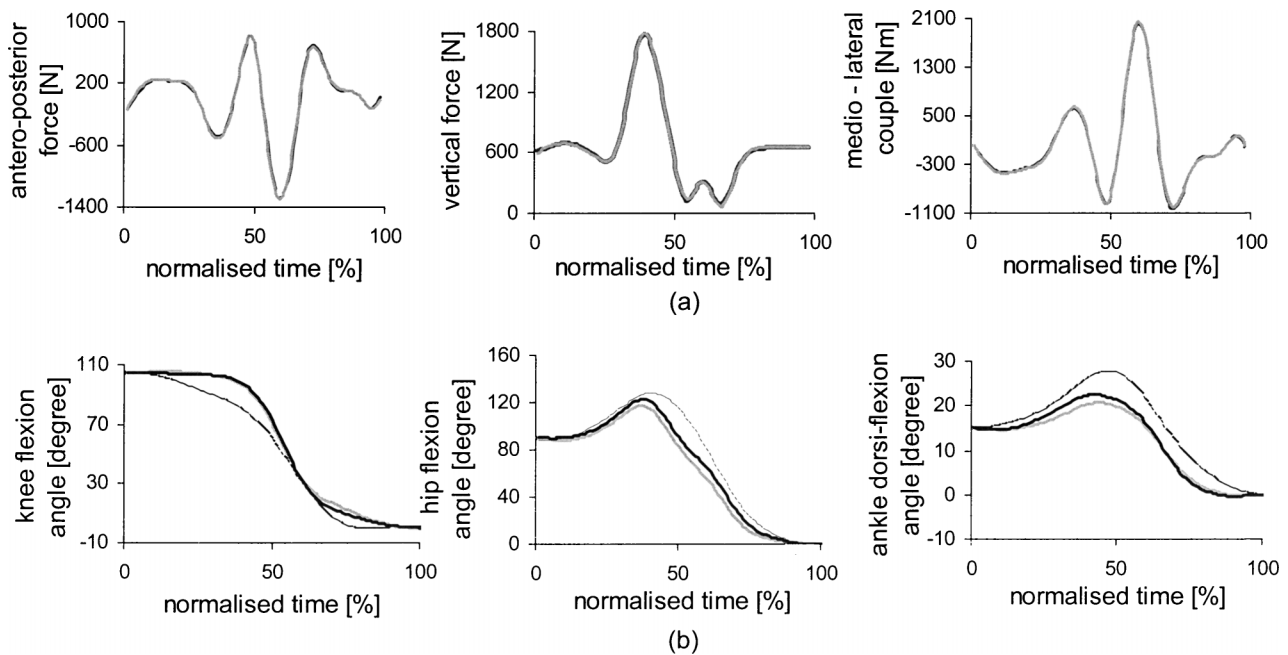


FIGURE 7. JAGO kinetic (a) and kinematic (b) estimates (black line) compared with the relevant benchmark functions (grey line). First approximation functions (dashed line) are also reported. JAGO parameters were set at the following values: $M = 500$, $d = 13\%$, $\bar{c} = 0.93$, $k = 6$, and $N + 1 = 15$. The ground reaction estimates overlap with the relevant benchmark curves.

patterns of the FAFs and the actual joint angle functions is irrelevant if it is kept below 15%. Results repeatability problems are strongly reduced by increasing the value of M . The number of intervals of time by which the duration of the motor act is divided, and over which the optimization procedure is carried out, had a relatively small effect on the results.

The accuracy of the JAGO model estimates may be summarized as having values around 1 and 6% of the relevant peak to peak values for the lower limb joint kinetic and kinematic variables. These values may be regarded as very low if compared with the inaccuracies associated with the conventional approach which estimates kinematic variables using stereophotogrammetric data and intersegmental loads using both the latter data and measured external forces.^{4,5} It is, however, evident that if the JAGO model is used with measured external forces, the discrepancy between the mechanical model embedded in it and the real musculo-skeletal system comes into play. But it should also be emphasized that the same discrepancy affects the accuracy of the above-mentioned conventional approach.

In conclusion, if a motor act is analyzed that allows for the use of a simple mechanical model of the musculo-skeletal system, then the JAGO model, and the associated experimental approach, may compete with the more demanding approach which uses both dynamometry and stereophotogrammetry. Whether more complex mechanical models may be effectively used in conjunction with the JAGO model and, therefore, more complex

motor acts analyzed, needs to be demonstrated by further investigation.

ACKNOWLEDGMENTS

This study was co-funded by the Ministero dell'Istruzione della Università e della Ricerca and by the Istituto Universitario di Scienze Motorie, Roma, Italia. The contribution of the former students—Massimiliano Bignami, Elisabetta Papa, Giacomo Polci, and Rosita Stroppa—is gratefully acknowledged.

REFERENCES

- ¹Box, M. J. A new method of constrained optimization and a comparison with other methods. *Comp. J.* 8:42–52, 1965.
- ²Cahouet, V., M. Luc, and A. David. Static optimal estimation of joint accelerations for inverse dynamics problem solution. *J. Biomech.* 35:1507–1513, 2002.
- ³Cappozzo, A. Minimum measured-input models for the assessment of motor ability. *J. Biomech.* 35:437–446, 2002.
- ⁴Cappozzo, A. Three-dimensional analysis of human walking: Experimental methods and associated artifacts. *Hum. Mol. Sci.* 10:589–602, 1991.
- ⁵Challis, J. H., and D. G. Kerwin. Quantification of the uncertainties in resultant joint moments computed in a dynamic activity. *J. Sports Sci.* 14:219–231, 1996.
- ⁶Cox, M. G. The numerical evaluation of B-splines. *J. Inst. Maths Appl.* 10:134–149, 1972.
- ⁷Crosbie, J., R. D. Herbert, and J. T. Bridson. Intersegmental dynamics of standing from sitting. *Clin. Biomech.* 12:227–235, 1997.

- ⁸Davis, R. B., S. Öunpuu, D. Tyburski, and J. R. Gage. A gait analysis data collection and reduction technique. *Hum. Mov. Sci.* 10:575–587, 1991.
- ⁹de Boor, C. On calculating with B-splines. *J. Approx. Theory* 6:50–62, 1972.
- ¹⁰Eng, J. J., and K. S. Chu. Reliability and comparison of weight-bearing ability during standing tasks for individuals with chronic stroke. *Arch. Phys. Med. Rehabil.* 83:1138–1144, 2002.
- ¹¹Hatze, H. The fundamental problem of myoskeletal inverse dynamics and its implications. *J. Biomech.* 35:109–115, 2002.
- ¹²Ikeda, E. R., M. L. Schenkman, P. O. Riley, and W. A. Hodge. Influence of age on dynamics of rising from a chair. *Phys. Ther.* 71:473–481, 1991.
- ¹³Khemlani, M. M., J. H. Carr, and W. J. Crosbie. Muscle synergies and joint linkages in sit-to-stand under two initial foot positions. *Clin. Biomech.* 14:236–246, 1999.
- ¹⁴Kuo, A. D. A least-squares estimation approach to improving the precision of inverse dynamics computations. *J. Biomech. Eng.* 120:148–159, 1998.
- ¹⁵Levin, O., J. Mizrahi, and M. Shoham. Standing sway: Iterative estimation of the kinematics and dynamics of the lower extremities from force-plate measurements. *Biol. Cybern.* 78:319–327, 1998.
- ¹⁶Ozaki, H., and C. Lin. Optimal B-spline joint trajectory generation for collision-free movements of a manipulator under dynamic constraints. In: IEEE, International Conference on Robotic and Automation, Minneapolis, MN, 1996, pp. 3592–3597.
- ¹⁷Pai, Y. C., H. J. Chang, R. W. Chang, J. M. Sinacore, and J. L. Lewis. Alteration in multijoint dynamics in patients with bilateral knee osteoarthritis. *Arthritis Rheum.* 37:1297–1304, 1994.
- ¹⁸Pai, Y. C., and M. W. Rogers. Speed variation and resultant joint torques during sit-to-stand. *Arch. Phys. Med. Rehabil.* 72:881–885, 1991.
- ¹⁹Papa, E., and A. Cappozzo. Sit-to-stand motor strategies investigated in able-bodied young and elderly subjects. *J. Biomech.* 33:1113–1122, 2000.
- ²⁰Risher, D. W., L. M. Schutte, and C. F. Runge. The use of inverse dynamics solutions in direct dynamics simulations. *J. Biomech. Eng.* 119:417–422, 1997.
- ²¹Vaughan, C. L., J. G. Hay, and J. G. Andrews. Closed loop problems in biomechanics. Part I: A classification system. *J. Biomech.* 15:197–200, 1982.
- ²²Vaughan, C. L., J. G. Hay, and J. G. Andrews. Closed loop problems in biomechanics. Part II: An optimization approach. *J. Biomech.* 15:201–210, 1982.
- ²³Winter, D. A. *Biomechanics and Motor Control of Human Movement*. Wiley-Interscience, Toronto, Canada, 1990, pp. 51–74, 85–89.